

Ultrashort Laser Pulse Effects in Ocular and Related Media

W. P. ROACH, M.S., Ph.D., M. E. ROGERS, M.S., Ph.D.,
B. A. ROCKWELL, B.S., Ph.D., STEPHEN A. BOPPART,
B.S., M.S., CINDY D. STEIN, B.S., and
CRAIG M. BRAMLETTE, A.S.

ROACH WP, ROGERS ME, ROCKWELL BA, BOPPART SA, STEIN CD, BRAMLETTE CM. *Ultrashort laser pulse effects in ocular and related media*. *Aviat. Space Environ. Med.* 1994; 65(5, Suppl.): A100-7.

Relatively little experimental and theoretical data exist on the retinal hazards of ultrashort laser pulses operating in the visible and near infrared spectral regions. Because of potential nonlinear effects that can occur from high-peak irradiance, ultrashort laser pulses propagate from the cornea to the retina, we have developed four projects within our Ultrashort Pulse Effects program. First, we discuss preliminary ED50 threshold values for nanosecond (ns), picosecond (ps), and femtosecond (fs) single pulses for in-vivo ocular exposures in Dutch Belted Rabbits using pulses in the visible spectral region. Then we examine two experiments that study nonlinear absorption using water tubes and measure the nonlinear refractive index of ocular tissue using the Z-Scan technique. Finally, we determine laser-induced breakdown thresholds in ultrahigh purity water. These studies give reasonable estimates of the damage thresholds and insight into the biophysics of how ultrashort pulses interact with ocular media.

CURRENT LASER TECHNOLOGY has reached a point where ultrashort, sub-nanosecond, pulsed laser systems that operate in the visible and near infrared spectral regions are commercially produced and finding their way into the industrial, medical, and military field settings. At present, there exist no laser safety standards for the maximum permissible exposure (MPE) from such systems either at the national [ANSI Z-136.1 (2)] or Air Force [AFOSH 161-10 (1)] level, owing to insufficient experimental and theoretical threshold data. Extrapolation of MPE levels from longer pulse widths is inappropriate since the enormous peak powers, on the order of gigawatts, associated with ultrashort laser pulses are believed to induce new mechanisms for dam-

age in ocular media. Thus, no basis exists for the reliable prediction of damage thresholds when such mechanisms are operative. Without a defined safety standard and precedents to answer medical and legal questions with regard to potential personnel exposures to ultrashort laser pulses, many types of users (such as military commanders, researchers, and medical practitioners) may be constrained from using ultrashort laser pulse systems.

We have developed a series of experiments to explore the propagation of ultrashort pulses through the ocular media and their interaction with the retina leading, potentially, to retinal damage. Our propagation experiments study the nonlinear phenomena that are most likely to occur. When the magnitude of these effects has been determined, we can decide if the nonlinear optical phenomena are important in the study of retinal damage thresholds.

Biological Damage Thresholds

In this article we review our overall in-house program directed toward understanding retinal damage from sub-nanosecond pulses conducted during the past year and a half. Our ultimate goal is to determine the laser pulse energy incident at the cornea required to give a minimal visible lesion (MVL) or hemorrhagic lesion (HL) at the retina. However, owing to a lack of experimental data for retinal damage below 1 ns, new MVL data is crucial in order to gain a clear understanding of how to tailor our experiments. Our choice of subjects in this preliminary study is Dutch Belted Rabbits. Future studies will use Rhesus monkeys that more closely model human retina.

The few data points that do exist tend to confuse the issues surrounding retinal damage induced by sub-nanosecond laser pulses. For example, the observations of Birngruber, Puliafito, Gawande, Lin, Schoenlein, and Fujimoto (3) that supra-threshold exposures in

From the Armstrong Laboratory, Occupational and Environmental Health Directorate, Optical Radiation Division, Brooks AFB, TX.

Address reprint requests to: W. P. Roach, Ph.D., who is AFOSR Technical Manager for the project, Armstrong Laboratory, Optical Radiation Div., 8111 18th St, Brooks AFB, TX 78235-5215.

Chinchilla Gray Rabbits up to 100 times threshold using 80-fs pulses at 625 nm yield only lesions of no greater severity than threshold, are indicative of a self-limiting process mediated by transmission of ultrahigh irradiance pulses through the eye. Further, such observations are also representative of nonlinear effects like two-photon absorption, self-focusing, or laser-induced breakdown (LIB). Thus, we have aimed our research program to investigate these phenomena in ocular tissue.

Preliminary studies were undertaken to measure the laser pulse energy required to give an MVL in Dutch Belted Rabbits using pulse durations from 5 ns to less than 100 fs in the visible region of the electromagnetic spectrum (19). The 50% probability for MVL (ED_{50}) thresholds were determined in these subjects using probit analysis (8), and we report for the first time independent verification of the Birngruber et al. data (3). Table I and Fig. 1 summarize the results of the preliminary threshold studies. We note that the 90-fs, 580-nm exposure in our study compared extremely well to that of Birngruber et al. We observe a comparable retinal damage threshold and concur with their observation that exposures in excess of 100 times threshold do not result in hemorrhagic lesions.

Both comparable observations remain perplexing in that visible wavelength Q-switched and mode-locked laser pulses usually result in hemorrhagic lesions with exposure doses ranging from 2 to 10 times the corresponding retinal damage threshold (4). We postulate that ocular focusing of the incoming laser pulse results in the LIB threshold being achieved at or slightly in front of the retinal focal plane. A rough order-of-magnitude estimate for breakdown can be made. Sacchi (15) reports a breakdown threshold in calf vitreous of about 10^8 V/cm. This corresponds to an irradiance of about 10^9 W/cm² using the relation $I = \epsilon_0 c E^2/2$. We consider an input beam, of 1 μ J, 100 fs in duration, and a 0.385 cm² area (7-mm diameter pupil). This pupil size yields approximately 3×10^7 W/cm². The eye focuses the beam so that a gain of about 10^5 results. Thus, the focal irradiance is about 10^{12} W/cm², exceeding breakdown threshold by a sufficient margin to make plasma formation highly likely. Indeed, the location of the event may be well in front of the retina. Therefore, the resultant "shielding" and energy dispersal due to LIB formation at the breakdown site in the vitreous attenuates the forward propagation of laser pulse energy so that rupture of choroidal blood vessels is avoided.

TABLE I. MVL THRESHOLD VALUES DETERMINED OPHTHALMOSCOPICALLY FOR DUTCH BELTED RABBITS AT THE 95% CONFIDENCE LIMIT USING PROBIT ANALYSIS.

Laser Pulsewidth	Laser Wavelength	MVL Thresholds (1 h, μ J)	Variance (μ J) (95% Level)
4 ns	532nm	4.97	(3.49–6.55)
50 ps	532nm	4.90	(3.20–7.00)
5 ps	580nm	2.57	(2.26–2.86)
500 fs	580nm	0.95	(0.83–1.06)
90 fs	580nm	1.01	(0.77–1.23)

METHODS AND RESULTS

Nonlinear Optical Properties of Ocular Media from 5 ns to 100 fs

The aim of our work in nonlinear optical properties, carried out in parallel with our in-vivo studies, has been the determination of such properties in ocular and related media. This effort involves the development of new experiments that characterize the onset of nonlinear phenomena as a response to high intensity fields (gigawatt or greater peak powers per pulse) generated by ultrashort laser pulses. We examine three phenomena: nonlinear absorption, self-focusing, and laser-induced breakdown. If the nonlinear absorption is significant as the laser pulse propagates from the cornea to the retina, then the retinal irradiance would be reduced below the value we would estimate based on linear propagation theory. Self-focusing, resulting from a positive nonlinear index of refraction, can cause the laser beam to collapse to a filament and greatly increase the irradiance. The study of LIB is important because it potentially mediates retinal damage. We report theoretical and experimental modeling of nonlinear absorption for ultrahigh purity water as a baseline model for laser propagation in ocular media, measurement of the nonlinear refractive index, n_2 , for highly dispersive liquids as well as ocular tissue, and threshold measurements for LIB in ultrahigh purity water*. All experiments reported here have been conducted in the spectral region from 400 to 1,064 nm, using both continuous wave (CW) and pulsed laser sources operating in the ns, ps, and fs time domains.

Linear and Nonlinear Propagation in Ultrahigh Purity Water

To develop a reasonable model that would allow prediction of the onset of nonlinear events (e.g., nonlinear absorption) induced in ocular tissue from subnanosecond laser pulses, ultrahigh purity water is studied as the propagation media. It is well understood that the linear response, that is the linear attenuation in the region of 400 to 1,064 nm, for ocular tissue is very much water-like (10). To extend our understanding into the nonlinear absorption regime, we use a Michelson type optical setup (13,14) shown in Fig. 2. Either CW or pulsed laser sources may be used for a range of field intensities to be propagated through reference and sample water tubes, and attenuated irradiances collected using PIN10 diodes on a fast sampling oscilloscope. The ratio of intensities can be expressed as a function of path length and attenuation modeled using Beer's Law.

We now develop some theoretical relationships that we can use to analyze the results of the water tube experiments in order to determine the nonlinear absorption coefficient. Beginning with Maxwell's equations for plane electromagnetic waves, the linear absorption coefficient can be written as $\alpha = 2\omega k/c = 4\pi k/\lambda = -(1/I)dI/dz$, indicating the dependence on wavelength

*The ultrahigh purity was obtained from VLSI. The conductivity was 18.0 M Ω /cm and the water had parts per billion concentration in O₂, N₂, and CO₂.

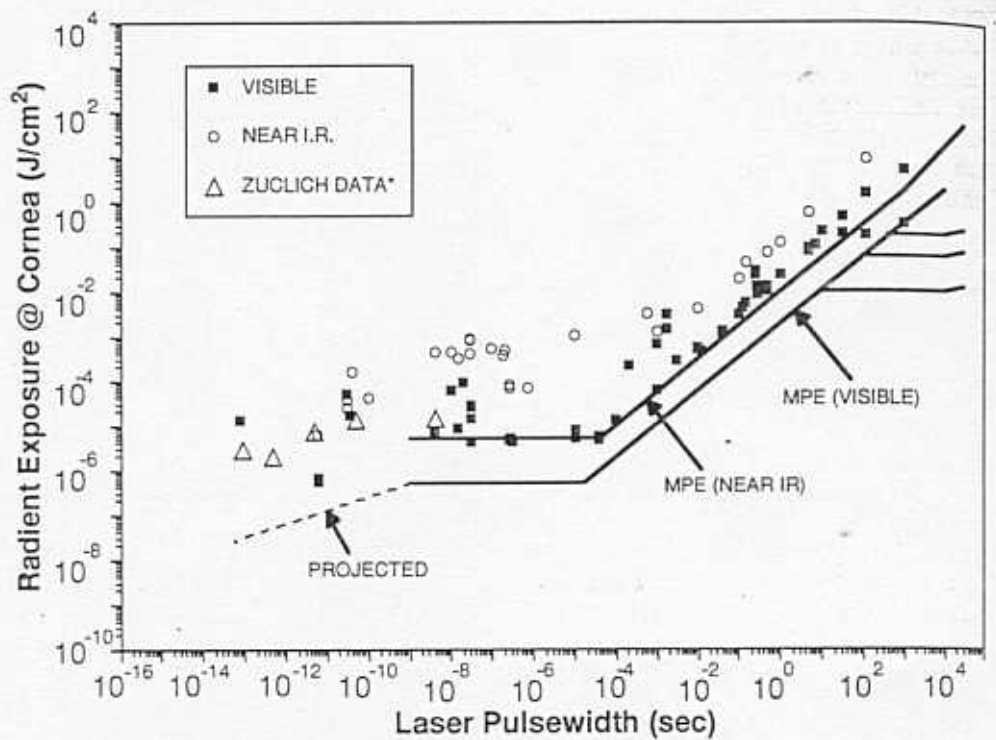


Fig. 1. Preliminary Dutch Belted Rabbit data compared with ANSI Z-136.1 [*Ref. 19].

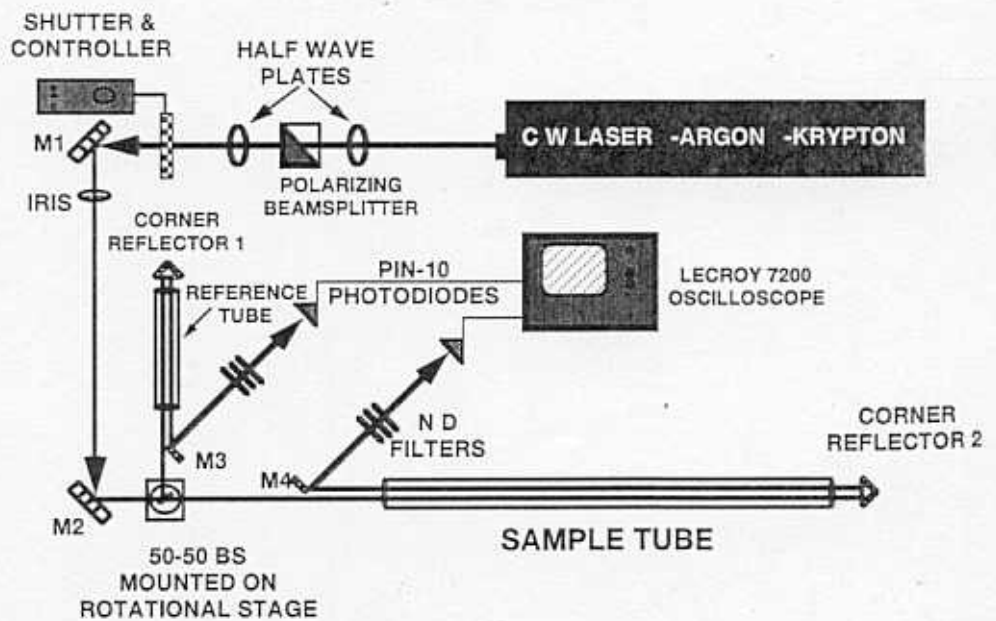


Fig. 2. "Michelson" type setup used to measure the ration of irradiances emerging from the reference and sample tubes of ultra-high purity water.

in this coefficient. This model, however, is valid far from any wavelengths that are strongly absorbed by the medium. Using this, we can express the attenuation of a laser beam with irradiance $I(z)$ after passing through a medium with an absorption coefficient α and a length z as:

$$I(z) = I_0 e^{-\alpha z} \quad \text{Eq. 1}$$

formally known as Beer's Law (12:85). The experimental design is shown in Fig. 2, where the length of the reference tube (z_1) is much less than the sample tube length (z_2). Noting that the optical path length is twice the tube length, then the irradiances after passing through the tubes are $I_1 = I_0 e^{-\alpha(2z_1)}$ and $I_2 = I_0 e^{-\alpha(2z_2)}$.

Taking the ratio of output intensities, we obtain $I_2/I_1 = e^{-2\alpha(z_2 - z_1)}$. Solving for the linear absorption, we arrive at:

$$\alpha = \frac{1}{2(z_2 - z_1)} \ln \left(\frac{I_1}{I_2} \right) \quad \text{Eq. 2}$$

At this point we want to include the effects of nonlinearity. Following Milonni and Eberly (13:680), we modify the differential equation that leads to Eq. 1 to account for nonlinear or two-photon absorption:

$$\frac{dI}{dz} = -\alpha I - \beta I^2 \quad \text{Eq. 3}$$

Here, α and β are the linear and nonlinear absorption of the media, respectively. Solving Eq. 3 for the irradiance, I , we obtain:

$$I = I_0 e^{-\alpha z} / [1 - (\beta I_0 / \alpha) (e^{-\alpha z} - 1)] \quad \text{Eq. 4}$$

Now that we have an expression for the irradiance as a function of both the linear and nonlinear absorption terms, we return to our experimental design. Using Eq. 4 and taking the ratio of the intensities after the laser beam transits the water tubes twice, yields:

$$\frac{I_2}{I_1} = e^{-2\alpha(z_2 - z_1)} \frac{\left[1 - \frac{\beta I_0}{\alpha} (e^{-2\alpha z_1} - 1)\right]}{\left[1 - \frac{\beta I_0}{\alpha} (e^{-2\alpha z_2} - 1)\right]} \quad \text{Eq. 5}$$

Using the idea of an "effective absorption" in Beer's Law, Eq. 1, we write $I = I_0 \exp(-\alpha_{\text{eff}} z)$ or $\alpha_{\text{eff}} = -(1/z) \ln(I/I_0)$. By analogy with Eq. 2, we obtain an approximate expression for α_{eff} in terms of the experimentally measurable ratio:

$$\alpha_{\text{eff}} = \left[\frac{1}{2(z_2 - z_1)} \right] \ln \left(\frac{I_1}{I_2} \right) \\ = \alpha + \frac{1}{2(z_2 - z_1)} \ln \left\{ \frac{\left[1 - \frac{\beta I_0}{\alpha} (e^{-2\alpha z_2} - 1)\right]}{\left[1 - \frac{\beta I_0}{\alpha} (e^{-2\alpha z_1} - 1)\right]} \right\} \quad \text{Eq. 6}$$

Plots of Eq. 5 and 6 for representative values of α and β are given in Fig. 3 and 4, where α is given in the literature (13) and β had been chosen arbitrarily. These equations allow us to make some predictions as to when the onset of nonlinear absorption will occur as a function of input irradiance using our experimental design. For example, in Fig. 4, we expect deviation from linearity to be achieved when the input irradiance is at or exceeds approximately 10^4 W/cm^2 . Recent studies have indicated an upper bound on the value for β of about 10^{-11} cm/W . This value moves the point at which the linear and nonlinear curves deviate to a higher value of input irradiance. Thus, higher peak power pulses would be required to observe nonlinear absorption. To date,

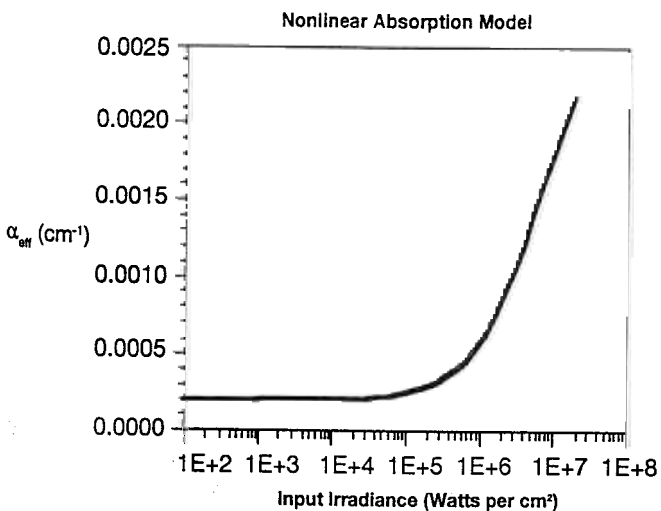


Fig. 3. The onset of the nonlinearity occurs between $1E4$ and $1E5 \text{ W/cm}^2$ using $\alpha = 2E - 4 \text{ cm}^{-1}$ and $\beta = 5E - 10 \text{ cm/W}$.

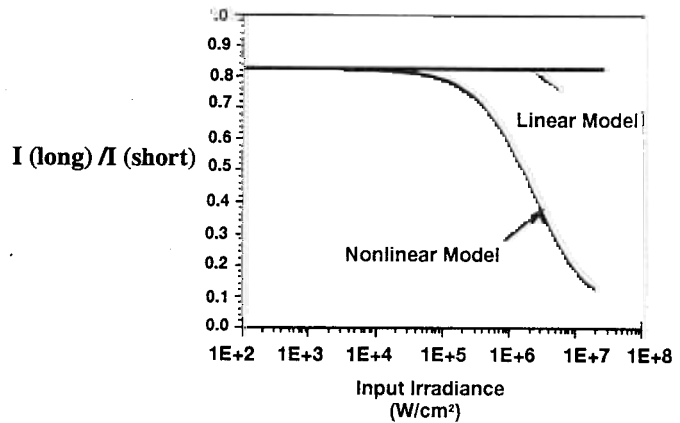


Fig. 4. Ratio of output irradiances are compared with linear and nonlinear absorption cases using $\alpha = 2E - 4 \text{ cm}^{-1}$ and $\beta = 5E - 10 \text{ cm/W}$.

the water tube experiments have been used in the linear region, giving excellent agreement with published linear absorption data. The high peak power pulse experiments will be performed next to assess the two-photon absorption.

Nonlinear Optical Property Characterization in Ocular Media: Z-Scan

Sub-nanosecond laser pulses possess peak powers that are well known to affect beam propagation in highly transparent materials (17). Self-action phenomena such as self-focusing or self-defocusing may, therefore, play a significant role in the damage induced at the retina (3,19). To assess the effects of nonlinear propagation in ocular media and on retinal damage, a sensitive yet accurate method of determining the nonlinear refractive index, n_2 , for ocular tissue was required. The technique of choice was Z-Scan (16), originally developed for the measurement of the optical nonlinearities observed in materials such as semiconductors and transparent optical crystals. In a logical extension of its use we have modified the technique to include the measurement of low n_2 aqueous and related biological media like cornea, lens, aqueous humor, and vitreous humor. Fig. 5 shows the Z-Scan optical configuration, where an incident pulsed laser beam passes through a thin focusing lens, through a 2.52 mm quartz cell containing our samples (sample length of 1.0 mm), and is collected at Detector 2 after passing through a preset aperture.

With self-action effects, such as self-focusing or self-defocusing, the radial changes in refractive index tend to collimate or decollimate the laser beam and increase or decrease the transmittance through the aperture as

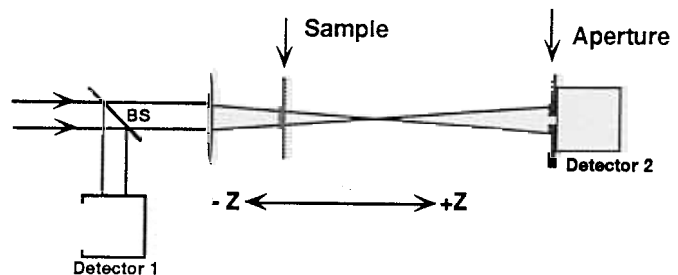


Fig. 5. Z-scan optical schematic.

the sample is translated through the focal plane of the lens in the $\pm z$ direction, respectively. The change in refractive index which gives rise to self-action effects is due to the nonlinear term, n_2 , from the equation $n = n_0 + n_2 I$, where n_0 is the linear refractive index and I is the beam irradiance for a Gaussian spatial distribution. Owing to self-action effects in the sample, the normalized transmittance spectrum recorded as a function of $\pm z$ is characterized by either a minimum-maximum (self-focusing) or maximum-minimum (self-defocusing) signature seen in Fig. 6. This characterization corresponds to positive and negative refractive nonlinearities.

We have measured the n_2 for human vitreous humor, rabbit vitreous humor, ultrahigh purity water, and physiological saline using 60 ps pulses at 532 nm. Our results are shown in Table II. The values in Table II represent the mean and SEM for multiple scans of each sample and represent pulse-to-pulse and day-to-day fluctuations in the laser characteristics. Nonlinear refractive index values for water have been previously measured by Smith, Lui, and Bloembergen (18), who found n_2 to be $(1.7 \pm 0.9) \times 10^{-13}$ electrostatic units (esu), well within experimental agreement of our value for water obtained using the Z-Scan technique [the error bar given in reference (18) is reported as an experimental uncertainty]. Fig. 7 shows typical Z-Scan spectra for human vitreous and rabbit vitreous. The data used in the plots are the result of 30 or more measurements at each z location in order to obtain statistically valid results for the sign and magnitude of the nonlinear index of refraction. We measured the well-known nonlinear index of refraction of carbon disulfide with our apparatus in order to baseline the experiment and obtained excellent agreement with published data (16). We conclude that given sufficient irradiance levels, self-focusing can occur which may either limit the density of energy that arrives at the retina or increase the likelihood of LIB. The location of the LIB event may occur well in front of the retina, limiting retinal damage. This is consistent with the lack of hemorrhagic lesions observed in our study and that of Birngruber. However, no direct observation of LIB has been made during a retinal exposure.

Optical Breakdown Localization and Analysis

Laser pulses operating in the ps and fs time domains are well known to permit threshold intensities for laser-induced breakdown (5,9) with significantly lower pulse energies than those permissible with ns pulse durations.

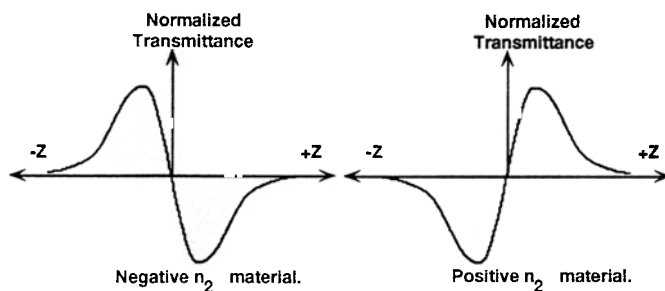


Fig. 6. Typical spectra from Z-scan experiments.

TABLE II. NONLINEAR REFRACTIVE INDEX VALUES MEASURED USING 60 PS AT 532 NM.

Material	n_2 (esu)
	$(1.4 \pm 0.4) \times 10^{-13}$
	$(2.7 \pm 0.6) \times 10^{-13}$
	$(1.3 \pm 0.6) \times 10^{-13}$
	$(1.8 \pm 1.3) \times 10^{-13}$

Among the physical processes which are believed to occur after LIB are plasma formation, acoustic and shockwave generation, and cavitation (6,7,11). In typical ophthalmic surgical applications, an Nd:YAG pulsed laser operating at 1064 nm with 7 to 10 ns pulses is capable of delivering 15 mJ per pulse, resulting in a desired LIB which is highly destructive to frail biological tissue.

Ultrashort, collinear propagating laser pulses incident upon the cornea and focused through the eye onto the retina offer a high degree of probability that LIB will occur, mediating the damage at the retina. We present preliminary studies on LIB in ultrahigh purity water as the media model for the eye. We discuss the effects laser pulse characteristics, media impurities, and LIB "shielding" may have on mediating retinal damage, and present the measured 50% threshold for LIB in ultrahigh purity water.

Spatial and temporal profiles, as well as energetics of each laser pulse, contribute to the overall characteristics of LIB in ocular media. Fig. 8 shows the optical schematic used in our study where 10-ns, 1064-nm single pulse events are focused into ultrahigh purity water using a 17-mm focal length lens. Spatial profiles of plasma formations are captured and digitized with a charge-coupled device (CCD) camera and beam-profiling software. The position (relative to the lens), intensity, and area of each single pulse initiated LIB event are recorded for varying laser pulse characteristics. We find that the most intense portion of the LIB event does not occur consistently at the focal point of the lens, but varies with the inherent energy fluctuations of the output from the laser as well as local impurity concentration within the target sample. Further, as pulse energy increases above breakdown threshold, LIB formations become larger both in area and elongation along the back-scattering direction of pulse propagation.

One of the fundamental properties of LIB is its target mediated threshold. Several factors that must be considered in determining the 50% probability of LIB are liquid type, impurity concentration, temperature, cone angle of the focusing lens used, spot size achieved from the lens, pulse duration, and energy of the pulse. The breakdown threshold for ultrahigh purity water is given as a comparison with work by others in Table III (7,15,20). Differences between experiments must be considered. Our irradiance threshold is an order of magnitude higher than those reported by Zysset, Fujimoto, and Deutsch (20), where deionized water was used that contained a higher concentration of impurities when compared with the ultrahigh purity water used in our work. We conclude, therefore, that if liquid type, focusing lens characteristics, temperature, and pulse charac-

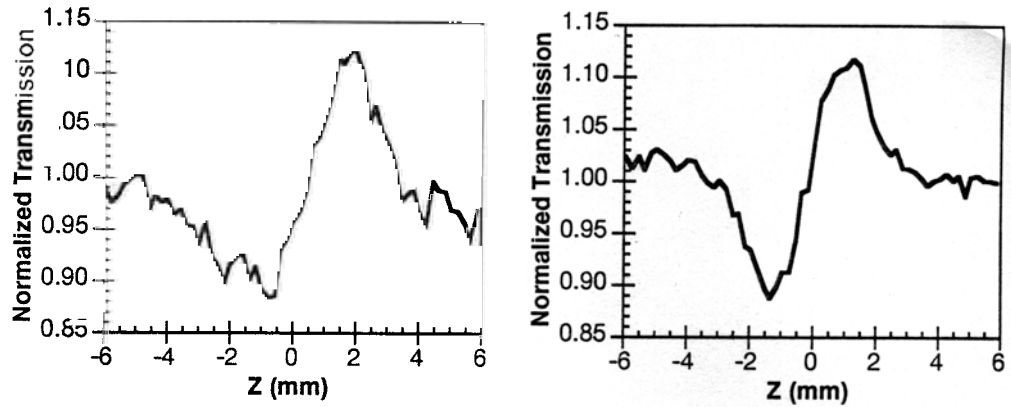


Fig. 7. Z-scan spectra obtained for human and rabbit vitreous humor. Both spectra use 28μJ with 532-nm pulses at 62 ps.

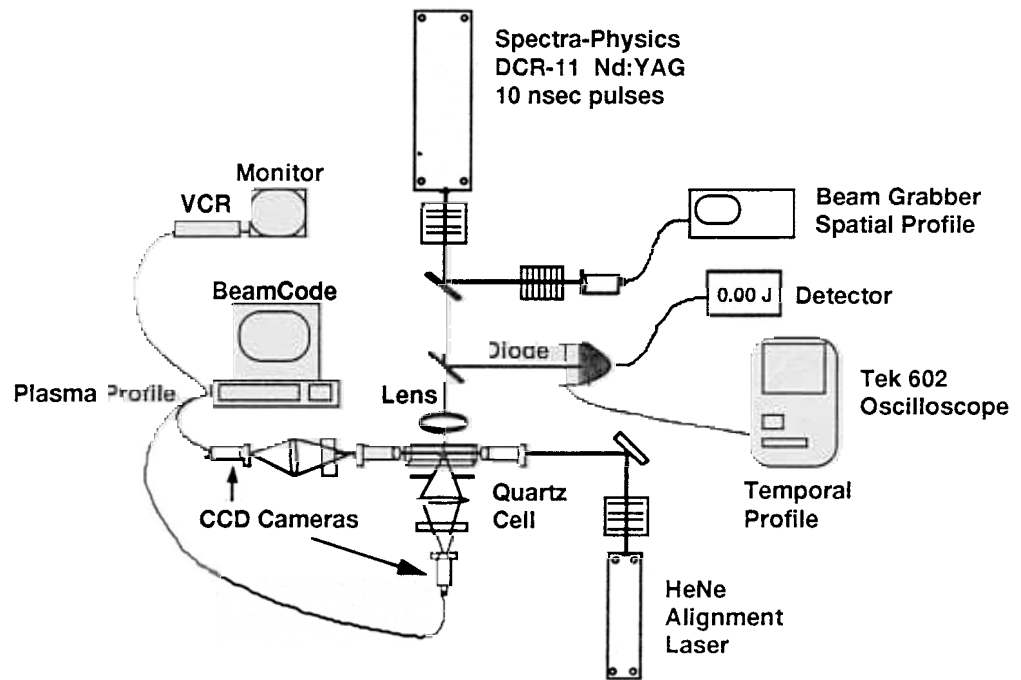


Fig. 8. Optical schematic for laser induced breakdown experiments.

TABLE III. THRESHOLD FOR LASER INDUCED BREAKDOWN IN WATER.

Source	Wavelength (nm)	Duration (ns)	Spot Size (μm)	Irradiance (W/cm ²)
Sacchi ^a	1064	75	75	3.45E10
Docchio, et al. ^b	1064	50	50	3.00E10
Zysset, et al. ^c	1064	4	4	32.0E10
Boppart ^d	1064	3.6	3.6	325E10

Note: Sacchi, Docchio used distilled water, Zysset used deionized, and Boppart used ultra-high purity (18MΩ/cm, once degassed).

(a) Sacchi, CA, J. Opt. Soc. Am. B, Vol. 8, No. 2, Feb 1991.

(b) Docchio, F, et al, Lasers in the Life Sciences, 1(2), 1986.

(c) Zysset, B, et al, Appl. Phys., B 48, 1989.

(d) Results of our research group at Armstrong Laboratory.

teristics are maintained as relative constants, then LIB events that occur in transparent ocular media are predominantly mediated by impurity concentration.

Another property of LIB in ocular media, associated with ophthalmic surgery (11), is that of "shielding." For example, the amount of energy per pulse used in surgery is well above the ANSI Z-136.1 and AFOSH 161-10 standards for safe laser exposures permitted for the retina.

A significant amount of this energy is consumed by the LIB event, therefore, preventing severe damage to the retina. However, LIB "shielding" effectiveness, even under the controlled skill of an ophthalmic surgeon, should never be considered a certainty. In Fig. 9 we show the results of measuring the throughput energy from 1,064-nm pulses beyond the LIB site in ultrahigh purity water. Experimentally, the "shielding" effectiveness is not 100%, and the measurable amount of energy propagating beyond the LIB site ($\geq 1E-4 J cm^{-2}$) is well above the permissible levels allowed at the cornea by the safety standards for this pulse duration and wavelength. We conclude, therefore, that LIB associated with ultrashort laser pulse exposures to the eye is not sufficient in itself to "shield" the retina from severe damage and in fact may be responsible for more catastrophic damage to the retina if they interact directly with this tissue.

SUMMARY AND CONCLUSION

The behavior of ns, ps, and fs pulses, in the visible to near infrared spectral regions, propagating from the cornea to the retina is still not thoroughly understood. We

ULTRASHORT LASER PULSE EFFECTS—ROACH ET AL.

8. Finney DJ. Probit analysis. 3rd ed. New York: Cambridge University Press, 1971.
9. Lauterborn W, Ebeling KJ. High speed holography of laser induced breakdown in liquids. *Appl. Phys. Lett.*, 1977, 31:663.
10. Maher EF. Transmission and absorption coefficients for ocular media of the rhesus monkey. Brooks AFB, TX: U.S. Air Force, 1978; USAFSAM-TR-78-32.
11. Martin NF, Gasterland DE, Rodriguez MM, Thomas G, Cummins CE. Endothelial damage from retrocorneal mode-locked neodymium-YAG laser pulses in monkeys. *Ophthalmology* 1985; 92(10):1376-81.
12. Milonni PW, Eberly JH. *Lasers*. New York: John Wiley & Sons, 1976.
13. Query MR, Cary PG, Waring RC. Split-pulse laser method for measuring attenuation coefficients of transparent liquids: application to deionized filtered water in the visible region. *Appl. Opt.* 1978; 17:3587.
14. Query MR, Wieliczka DM, Segelstein DJ. In: *Water (H₂O): handbook of optical constants of solids II*. Palik ED, ed. Boston: Academic Press, 1991.
15. Sacchi CA. Laser-induced electric breakdown in water. *J. Opt. Soc. Am. B.* 1991; 8:337.
16. Sheik-Bahae M, Said AA, Wei TH, Hagan DJ, VanStryland EW. Sensitive measurements of optical nonlinearities using a single beam. *IEEE J. Quant. Electron.* 1990; 26:760.
17. Shen YR. Self-focusing: experimental. *Prog. Quant. Electr.* 1975; 4:1-34.
18. Smith WL, P Liu, Bloembergen N. Superbroadening in H₂O and D₂O by self-focusing picosecond pulses from a Nd:YAG laser. *Phys. Rev. A.* 1977; 15:2396.
19. Zuclich JA, Elliott WR, Cain CP, Noojin GD, Roach WP, Rockwell BA, Toth CA. Ocular damage induced by ultrashort laser pulses. Brooks AFB, TX: Armstrong Laboratory; 1993; AL-TR-93-0099.
20. Zysset B, Fujimoto JG, Deutsch TF. Time resolved measurements of picosecond optical breakdown. *Appl. Phys.* 1989; 48:139.

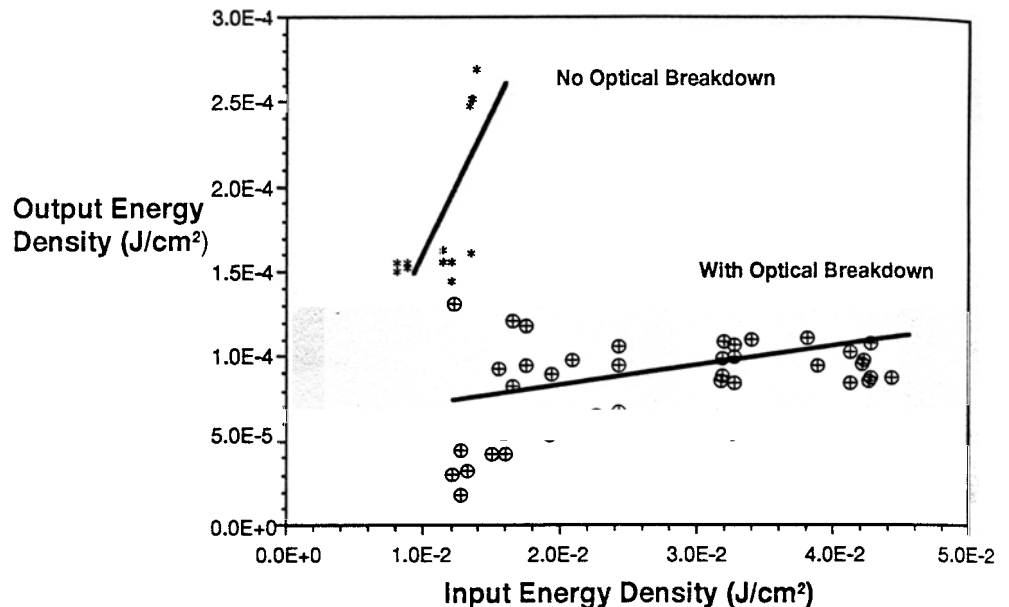


Fig. 9. Measurement of 1064-nm throughput after laser induced breakdown.

conclude from our preliminary in-vivo studies in Dutch Belted Rabbits that no HL's were produced using pulse energies up to 100 times threshold in agreement with Birngruber et al. (3). However, this study used an animal model that does not accurately model the human retina. Further research is planned using Rhesus monkey subjects. Also, from the MVL studies we observe a gradual trend toward lower energy densities required to produce threshold damage at the retina as pulse duration is decreased. Caution should be taken when interpreting interspecies data for MVL studies since numerous anatomical differences exist between Rabbits and Rhesus monkeys. However, we may still infer the downward trend which we expect to see when Rhesus subjects are studied and that data are included into the ANSI Z-136.1 standard. From our theoretical and experimental work, nonlinear optical effects are possible which may limit the energy density that reaches the retina, shift the focal plane anterior to the expected focal plane in the eye, or mediate the onset of LIB. We are still left with questions concerning the exact mechanisms which govern retinal damage when sub-nanosecond pulses are propagated through the eye. For example, does an LIB event occur in the eye at the pulse energy that creates an MVL? How much does self-focusing change the retinal irradiance in the eye? If the LIB event occurs anterior to the retina, how far will the resulting shock wave propagate? Will it cause retinal damage? How can histopathological studies help determine the mechanism of damage? The determination of the damage thresholds and the setting of Maximum Permissible Exposures are independent of understanding the mechanism of damage. However, such understanding is essential to extending the use of lasers in therapeutic applications where supra-threshold exposures at new wavelengths and/or pulse durations are required.

Our model for nonlinear absorption allows us to make some prediction of the onset of nonlinear behavior in ocular media, and, given sufficient irradiance levels, self-focusing can occur indicated by our measured values for the nonlinear refractive index in human vitreous.

Further, LIB studies have shown us that the "shielding" effect does not eliminate all of the potentially hazardous energy carried by a pulse and may thus lead to retinal injury. In fact, LIB may be one of the primary mechanism that initiates catastrophic retinal damage such as HL formation when the energy density from ultrashort laser pulses is sufficient and the LIB event occurs at the retina. Our research in the area of ultrashort laser pulse effects will continue to explore the damage thresholds, as well as the mechanisms behind retinal damage, with the goal of improved safety standards and improved applications of these laser systems.

ACKNOWLEDGMENTS

The animals involved in this study were procured, maintained, and used in accordance with the Animal Welfare Act, the "Guide for the Care and Use of Laboratory Animals" prepared by the Institute of Laboratory Animal Resources, National Research Council, and Protocol #RZV-9104.

This work was supported by AFSOR (#2312A101), the Armstrong Laboratory, and Contract F33615-88-C-0631.

REFERENCES

1. AFOSH Standard 161-10, Health hazards control for laser radiation. Washington, DC: Department of the Air Force, 1980.
2. ANSI Standard Z136.1-1986. American national standard for the safe use of lasers. New York: American National Standards Institute, Inc., 1986.
3. Birngruber R, Puliafito CA, Gawande A, Lin W, Schoenlein RT, Fujimoto JG. Femtosecond laser-tissue interactions. *IEEE J. Quant. Elect.*, 1987, 23:1836.
4. Blankenstein MF, Zuclich J, Allen RG, David H, Thomas SJ, Harrison RR. Retinal hemorrhage thresholds for Q-switched neodymium-YAG laser exposures. *Invest. Ophthalmol. Vis. Sci.* 1986; 27:1176.
5. Bloembergen N. Laser-induced electric breakdown in solids. *IEEE J. Quant. Elec.* 1974; 10:375.
6. Capon MRC, Mello J. ND:YAG lasers: a potential hazard from cavitation bubble behavior in anterior chamber procedures. *Lasers Ophthalmol* 1986; 1:95.
7. Docchio F, Dossi L, Sacchi CA. Q-Switched ND:YAG laser irradiation of the eye and related phenomena: an experimental study. *Lasers in the Life Sciences*, 1987; 1:87.